Microdiffraction Imaging

Jean Jordan-Sweet
IBM Research Division
Yorktown Heights, NY 10598
JLJS@US.IBM.COM

Introduction

Microdiffraction, the determination of crystalline tilt, mosaic, and/or lattice spacings using a sub- to several-micron-sized x-ray beam, has grown in popularity with the advent of high-brightness, insertion-device-based synchrotrons. Although third generation sources like the APS and ESRF boast sub-micron beamsizes and plenty of flux [1-2], second generation facilities like the NSLS are definitely capable of producing enough bright beam for many microdiffraction applications.

The X20 Beamlines at the NSLS are used for a variety of x-ray techniques, including high-resolution diffraction, reflectivity, grazing-incidence diffraction, and time-resolved diffraction. More than half of the beamtime is used by IBM scientists to study materials used in microelectronics manufacturing. In 1997, a special-purpose instrument was commissioned by I.C. Noyan and coworkers [3,4] to use several-micron-sized x-ray beams to investigate technological issues related to structure and strain in small features. Some of these issues include thermally- and electrically-induced failure in thin metal lines [5,6], defects in heteroepitaxial films like SiGe/Si [7,8], and interfacial strain in small metal features deposited on silicon due to thermal expansion mismatch [9]. Problems such as these require high brightness x-rays to obtain enough signal from the region of interest and to avoid unwanted signals from surrounding areas.

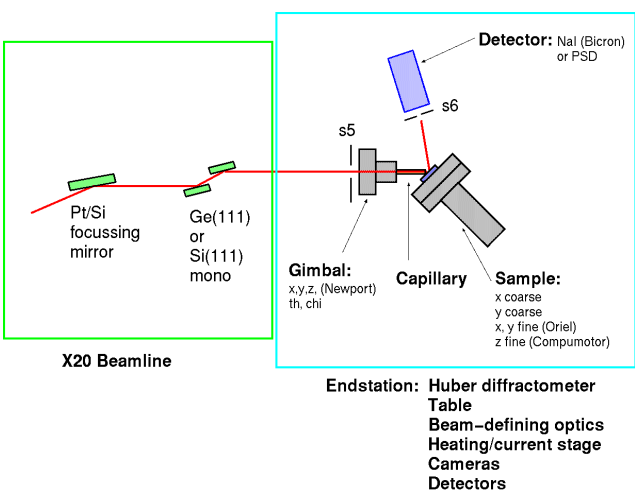

Figure 1: *Layout of X20A microdiffraction setup. (Not to scale).*

There are several ways to do microdiffraction. One can use a "white" or "pink" beam (i.e. radiation having a significant spectral range) and use an area detector, energy-dispersive detector, and sophisticated algorithms to determine the energy and diffraction angle for each reflection (the Laue technique). An advantage of this technique is the ability to hold the sample in a fixed position. Disadvantages are determining the energy of a reflection accurately enough, and indexing the reflections. In a clever modification of this style, at the APS G.E. Ice and coworkers have been able to insert a specially engineered scanning monochromator into the beam path to determine the energy of each reflection to within 2 eV [10]. Alternatively, one can use monochromatic radiation. Although the energy is well-known, here the challenge lies in aligning the sample and keeping it aligned over a range of orientation angles.

The X20 microdiffraction instrument uses a tapered capillary to condense monochromatic radiation onto the sample. A modified two-circle diffractometer with two arcs and a high-resolution scanning stage is used to orient the sample and position a single-channel detector to measure diffracted x-rays. In addition, transmitted beam intensity can also be measured, and fluorescence from the sample can be collected with a Si(Li) detector.

Instrumentation

Figure 1 shows the instrumental configuration. The X20A beamline has a dipole magnet source, a 1:1 toroidal focussing mirror, and a double-crystal Ge(111) monochromator. The beam is ~1mm in diameter at the entrance to the tapered capillary microbeam optic.

A photograph of the endstation is shown in **Figure 2**. The microdiffraction instrumentation is mounted

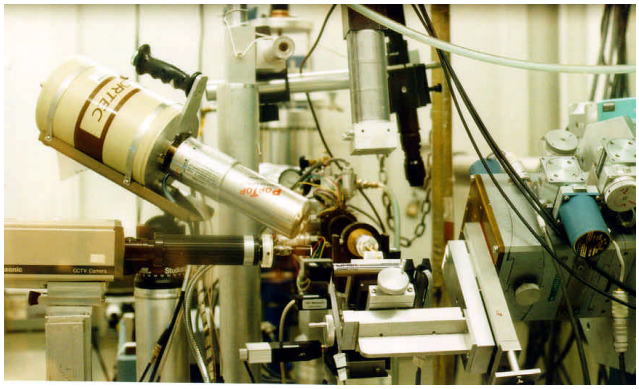

Figure 2: *Diffractometer, sample translation stages, cameras and Si(Li) detector.*

on a table which sits on kinematic floor mounts. The optics and diffractometer will be described in subsections below.

Optics

There are a number of ways that synchrotron beams can be shaped or focussed down to the size of microns. If one assumes that the source (bending magnet or insertion device) produces an essentially parallel beam, then a more condensing downstream optic will produce a more divergent (or convergent) focussed beam. Undulator beamlines at third-generation sources like the APS are bright enough that in some cases a pinhole can be used to define a microbeam with enough intensity to do the experiment [11]. However, more commonly, zone plates or Kirkpatrick-Baez mirrors are used to condition the beam. These two optics are relatively expensive, and have their own pros and cons. A third type of optic, the tapered capillary, is used at X20 (Schematic in **Figure 3**, photo in **Figure 4**).

Figure 3: *Schematic of x-rays passing through a tapered capillary.*

The capillaries used at X20 are fabricated in-house [12] and have inner surfaces tapered to approximate a parabola so that x-rays undergo several total external reflections off the inside walls and converge at a critical angle of $\sim 0.3^{\circ}$. The focus of the x-ray beam is extremely close to the tip of the capillary. This results in a working distance that is extremely short: about 0.5 – 1.5mm from the capillary tip to the sample surface. The divergence and spot size have been measured by knife-edge scans to be $\sim 0.35^{\circ}$ (6.1 mr) and from 2 to 20 μm in diameter, respectively. The FWHM of the x-ray beam from our "best" capillary, at a typical sample distance of 1.4 mm from the tip, is ~ 3 μm and the flux at 8.5 keV is $\sim 1.5\times10^{8}$ cts/sec. **Figure 5** shows the swirled shape of the beam exiting a typical capillary.

The footprint of the beam on the sample varies as $h/\sin(\omega)$, where h is the beam diameter and ω is the sample angle (usually $\omega = 2\Theta/2$) for the diffraction peak being measured. Since the beam profile is very non-uniform, special care must be taken in determining the "zero" of 2Θ and in interpreting diffraction peak shapes. In extreme cases a beam profile could deconvoluted from data to obtain true peak shapes.

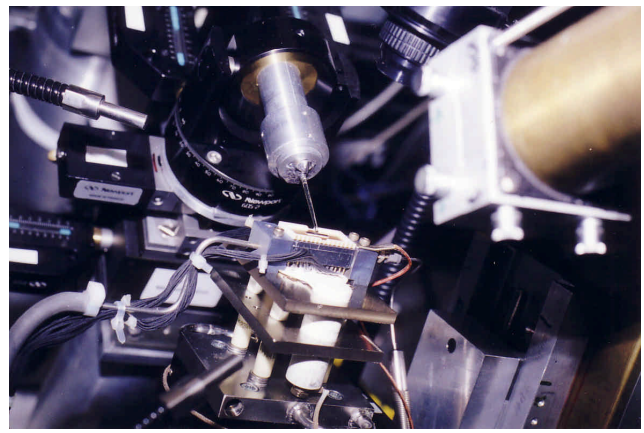

Figure 4: *Photograph of gimbal mount, capillary, and sample stage.*

The actual diffraction resolution is determined by three factors: the divergence of the incident beam, the acceptance of the sample, and the acceptance of the detector. In many of our experiments, we measure diffraction from single crystal silicon wafers or nearly perfect SiGe, which greatly narrows the angular resolution of the diffracted beam. Alternatively, by narrowing the receiving slits directly in front of the detector we can reduce the acceptance to under a tenth of a degree. A detailed description of experimental concerns regarding accuracy and resolution in monochromatic microdiffraction using tapered capillaries can be found in Reference 13.

Figure 5: *Polaroid photo of beam at the entrance to the detector.*

One trick for accurate determination of lattice spacings is to measure reflections at Θ angles as close to 90° as possible. At this angle the footprint is smallest and, according to Bragg's Law, the error in sinΘ caused by a given error in Θ is the smallest: $\Delta d/d$ = -cot $\Theta\Delta\Theta$ [14].

Diffraction Geometry

The diffractometer used at X20 has 0.5 μm-resolution x, y, and z sample-scanning stages mounted on a standard two-circle Huber diffractometer with partial χ and ϕ arcs. The arcs are mounted on translators so that all the diffractometer circles can be adjusted carefully to bring them into concentricity. Despite this, the "sphere-of-confusion" of the diffractometer cannot be reduced mechanically to less than tens of microns. Accordingly, a protocol for measuring and compensating for the ω, χ, and ϕ radii of confusion has been developed [15]. This is essential in cases where several diffraction peaks are to be measured at a specific location on the sample. It is imperative that the same region of interest is being illuminated at each diffraction angle. Basically, the position of a fluorescent marker or grid is measured as a function of angle for each circle, and a plot of x and y positons vs. angle is fit to an analytical expression which then tells how the translation stages should be moved to correct for the drift at any angle. This calibration must be performed after each realignment of the capillary or diffractometer. In many cases, where changes in the sample are measured at one diffraction position, or in scanning diffraction microtopography at only one angle, this extra care need not be taken.

The sample stage is a standard Newport optical stage, and can accommodate several special holders: one having f rotation, one with capability for heating and supporting wire-bonded test structures on Si wafers, and one with a four-point bending jig for stress experiments.

Data Collection

The X20 instrument has three modes of operation. One is diffraction imaging (scanning micro-topography), where the detector is moved to a reflection of interest, and the diffracted intensity is collected as the sample is rastered in the beam. This mode is used for grain mapping, defect imaging, strain contrast mapping, etc. Once a "mesh" has been made across a submillimeter-sized area, one can return easily to regions of high intensity and "tweak" them up, in preparation for more detailed measurement of lattice tilt, mosaic broadening, or lattice spacing. This is the second mode: standard diffraction analysis. For a silicon wafer at the Si(004) reflection angle of 32° θ (at 8.5 keV) the measured *d*-spacing repeatability is $\Delta d/d$ = 0.0003 [13]. The third mode of operation is fluorescence mapping, for which the sample again is translated in the beam and the fluorescence signal of interest is collected by a Si(Li) energy-dispersive detector. This is useful for mapping fluorescence markers or other features for alignment of the sample in the x-ray beam, and for measuring the sphere-of-confusion of the diffractometer.

Data Analysis

Data are collected using a special geometry code in the "spec" program [16] called "fourcM." Scans are stored as sequential stanzas of ascii data in files and can be converted to single files of columns of numbers using "c-plot" [16]. C-plot is also used to plot and analyze data as it is being collected. MCA spectra can be stored as individual data files, or regions of interest can be singled out and added as a column to the scan data file. The MCA software "spec" macros are freely available from the ESRF.

Examples

Strain Fields in Ni/Si Structures

I.C. Noyan[1], P.-C. Wang[2], S.K. Kaldor[1], J.L. Jordan-Sweet[1]

1. IBM Research Division, Yorktown Heights, NY
2. IBM Microelectronics Division, Hopewell Junction, NY

An illustration of the capabilities of this instrument (one that yielded unexpected results) was the study of interfacial strain caused by residual stresses in small Ni metallization features deposited on Si(111) [9]. In discrete thin-film features, the feature edges cause significant shear stresses/strains, unlike blanket films in which the stresses are biaxial and isotropic. The sample in this study consisted of an array of 190 μm diameter Ni pads, 1 μm thick, separated by 220 μm, deposited by vacuum evaporation onto a Si(111) substrate maintained at room temperature. To characterize the strain distribution, the Si(333) integrated diffraction intensity was mapped by step-scanning over an area containing several pads. Simultaneously, the Ni Kα fluorescence signal at 7.478 keV was recorded using a Si(Li) detector. The x-ray spot on the sample was an ellipse

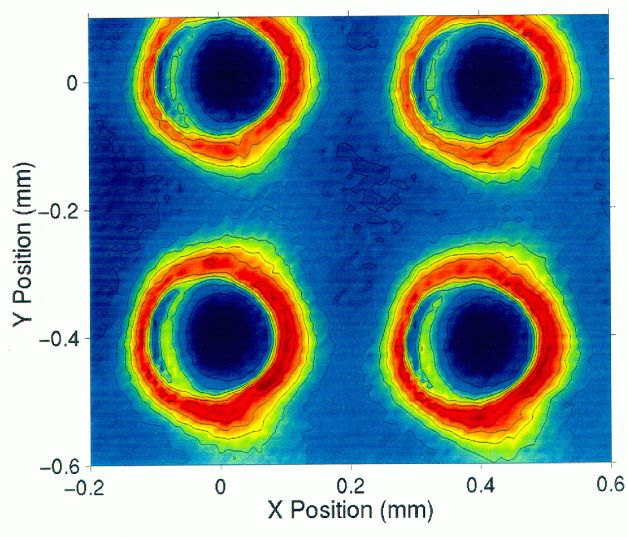

Figure 6: *Si(333) diffraction intensity map of Ni dots on Si substrate.*

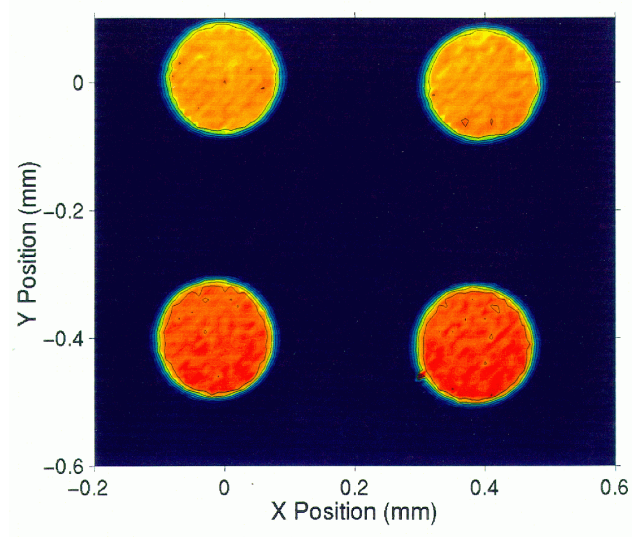

Figure 7: *Ni fluorescence from Ni dots on Si.*

14 μm in the direction parallel to the diffraction plane and 10 μm normal to it. **Figure 6** shows contoured area maps of the Si(333) diffraction intensity. **Figure 7** shows the Ni fluorescence signal collected simultaneously with the diffraction intensity over the same area.

Figure 6 is essentially a strain map of the Si substrate. When unperturbed, diffraction from a silicon substrate is dynamical, and is limited by extinction effects [17]. When the silicon lattice is strained, it becomes imperfect, extinction effects are eliminated, and the diffracted intensity increases. The smooth, blue regions correspond to relatively strain-free Si under or close to the Ni pads. The lack of intensity fluctuations under the pad demonstrated that the adhesion was uniform and good. The contours outside the pads correspond to the far-field strains induced in bare Si by the Ni, which appeared to be circularly symmetric.

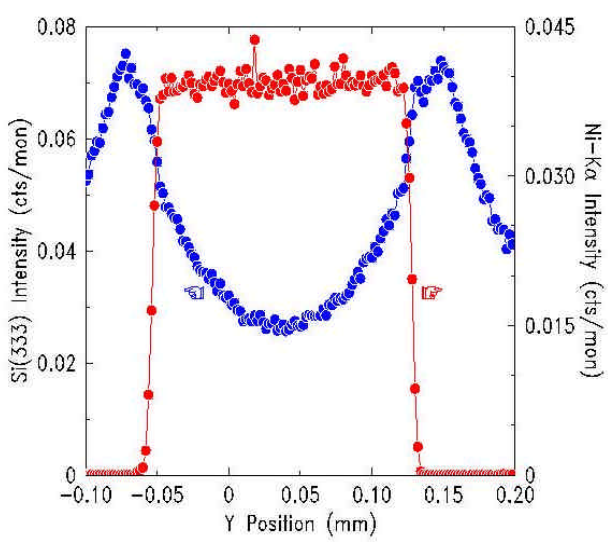

Figure 8: *High-resolution scan across one pad.*

Figure 8 shows a close-up profile scan across one pad. The blue circles corresponding to the diffraction intensity reached a maximum outside the edge of the fluorescence intensity (red circles). This surprising result showed that the position of maximum strain contrast is ~ 20 μm outside the edge of the Ni pad, contrary to results from analytical solutions and finite-element models of interfacial strain.

Real-time Characterization of Electromigration Effects in Al(Cu) Wires

P.-C. Wang[1], I.C. Noyan[2], S.K. Kaldor[2], J.L. Jordan-Sweet[2], E.G. Liniger[2], and C-K. Hu[2]

1. IBM Microelectronics Division, Hopewell Junction, NY
2. IBM Research Division, Yorktown Heights, NY

Electromigration is the redistribution (diffusion) of material induced by high electrical current densities in thin conducting lines. This diffusion sets up stress gradients along the line, and can cause a failure by forming voids at the cathode end and hillocks at the anode end. Electromigration has become a critical problem as interconnects have been scaled down to submicron widths with subsequently increased current densities. The addition of Cu solutes to Al-based interconnects dramatically increases their electromigration lifetimes.

Microdiffraction scanning topography has been used to measure the simultaneous evolution of electromigration-induced Cu concentration and stress

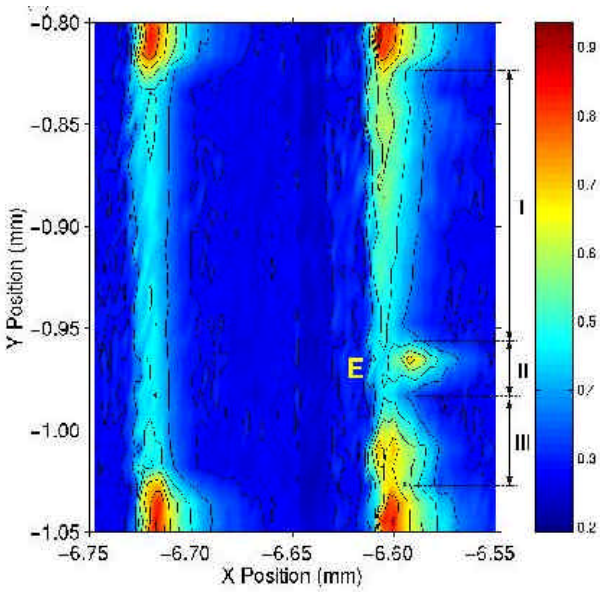

Figure 9: *Si(333) diffraction topograph of a pair of Al(Cu) lines.*

profiles in Al(0.25 at. % Cu) lines on a Si(001) substrate [6]. The Al(Cu) lines were 10μm wide, 200μm long, and 0.5μm thick, passivated with 1.5μm-thick SiO_2. The lines were terminated with W pads at both ends, which served as wire-bonding pads and blocking boundaries against mass flow. A pair of lines was measured, with one serving as a control (no applied current). Evolution of Cu distribution and local stress distributions were monitored in real time by repetitive scans at different locations across the conductor lines before and during current passage. Both Si(004) diffraction and Cu Kα fluorescence were collected simultaneously. The Si(004) intensity provides topographic information at the film/substrate interface, which is related to and scales with the local stress in the conductors [5,17,18]. **Figure 9** shows log scale intensity contours for a raster scan of Si(004) diffraction from a control line (left) and line that had been stressed at $1x10^5 A/cm^2$ for about 19 hours at 302°C prior to the measurement (right).

The intensity contours of the control line stay uniform over the length of the line, indicating that it is stress free and has a uniform distribution of Cu. The high intensity at the ends of the lines in **Figure 9** are caused by high intrinsic stress in the W pads. For the electromigrated wire, the Si(004) intensity was enhanced in region I near the cathode due to increase in

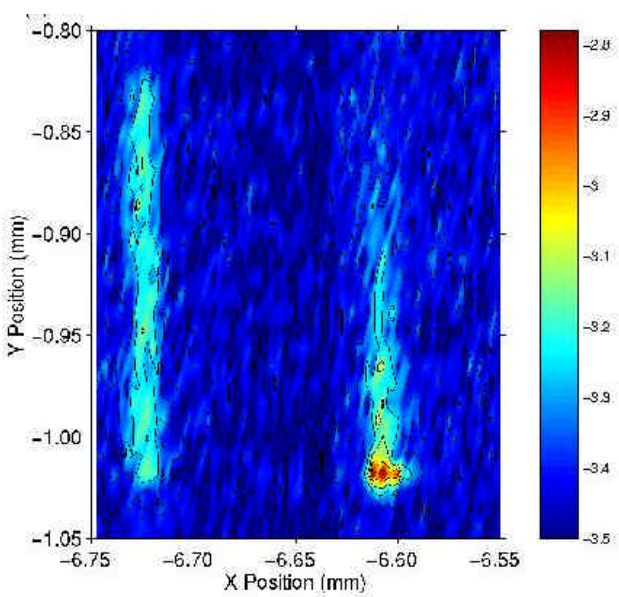

Figure 10: *Cu fluorescence map of Al(Cu) two lines.*

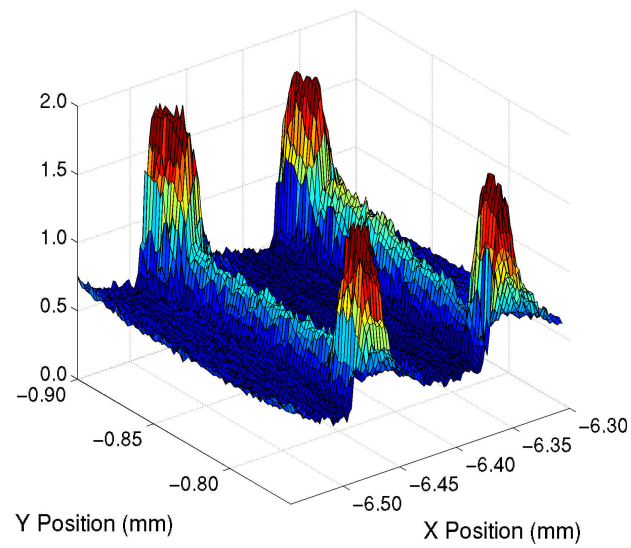

Figure 11: *Topograph of control and electromigration-stressed Al lines.*

tensile stress. The stress gradient is interrupted at position E in region II, and the Si intensity again increases at the anode end in region III, as a result of local compressive stress from the mass pileup there. The intensity at E increased with time. Post-experimental optical microscopy revealed a lateral metal extrusion embedded between the passivation and the substrate. Interestingly, the area surrounding the extrusion appeared to be similar to that of the control, and thus nearly stress-free. The extrusion may have relieved the compressive stress in the adjoining sections. **Figure 10** shows a gradient in Cu concentration along the line, with concentrations below that of the control at the cathode, and above that of the control at the anode.

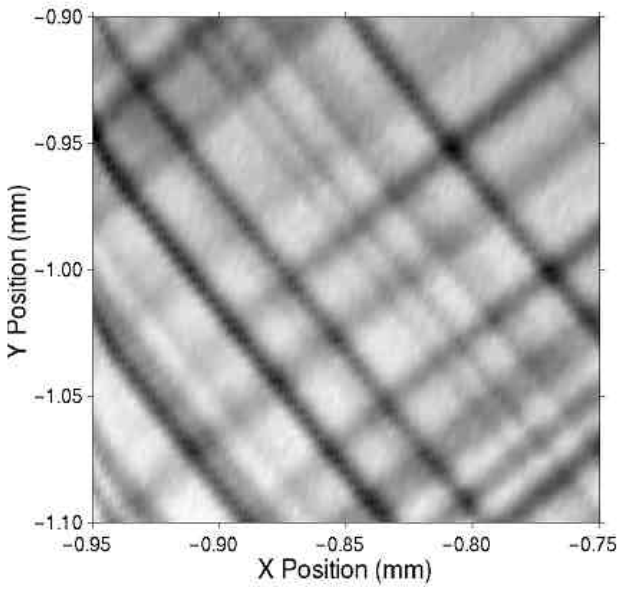

Figure 12: *Scanning x-ray microtopograph of 0.5% strain-relaxed SiGe/Si (15% Ge).*

Figure 11 shows Si(004) intensity contours for a pair of unpassivated, 10μm-wide Al lines plotted as a 3D surface mesh [5].

The high intensity at the ends is again due to stress in W pads. The control line, on the left, is uniform along its length. The line on the right was measured after 11 hours at 258°C and $4x10^4$A/cm^2 current density. A linear stress gradient can easily be seen, with the stress decreasing towards the cathode end. Measurements of lines having lengths from 50 to 200μm show that the maximum stress gradient is inversely proportional to length. This experiment also measured the lowest current densities to date at which strain appears.

Scanning X-ray Microtopographs of Misfit Dislocations at SiGe/Si Interfaces

P.M. Mooney, J.L. Jordan-Sweet, and J.O. Chu

IBM Research Division, Yorktown Heights, NY

SiGe is under consideration as a substrate for strained-silicon conduction channels in future CMOS Field Effect Transistors [19]. Strain-relaxed SiGe is grown via UHV-CVD on Si(001) wafers by step-grading up in Ge concentration by ~5% per step to the desired top layer composition (usually ~30%). By this method, the misfit strain between layers is always small, and for films above the critical thickness for relaxation, results in strain relaxation by dislocation multiplication and glide which forms long misfit dislocations, rather than roughening and random misfit dislocation nucleation. The dislocations glide downwards and threading arms annihilate, leaving the upper SiGe surface smooth and with a low concentration of threading defects.

Scanning microdiffraction topography has been used to study the distribution and characteristics of misfit dislocations in SiGe films ranging from unrelaxed (few or no dislocations) to fully relaxed (many dislocations). Variations in the Si(004) diffraction intensity yield information about the perfection of the Si wafer substrate, and variations in the SiGe(004) diffraction intensity yield information about the defect structure of the SiGe film. **Figure 12** shows a scanning topograph of a 459nm thick $Si_{0.85}Ge_{0.15}$/Si film that is 0.5% relaxed [8].

The layer topograph has dark lines where there are strain fields due to pileups of misfit dislocations at the interface, running along <110> directions. The bright diffracting areas are regions where the crystal is not tilted or distorted by any strain fields. "Line" scans across the x direction at the SiGe(004) reflection condition and the Si(004) reflection condition in **Figure 13** show complementary behavior. Diffraction intensity from the substrate actually increases in areas where there is a distortion because of the elimination of extinction in the otherwise "perfect" Si crystal. (i.e. the scattering becomes kinematic rather than dynamic)

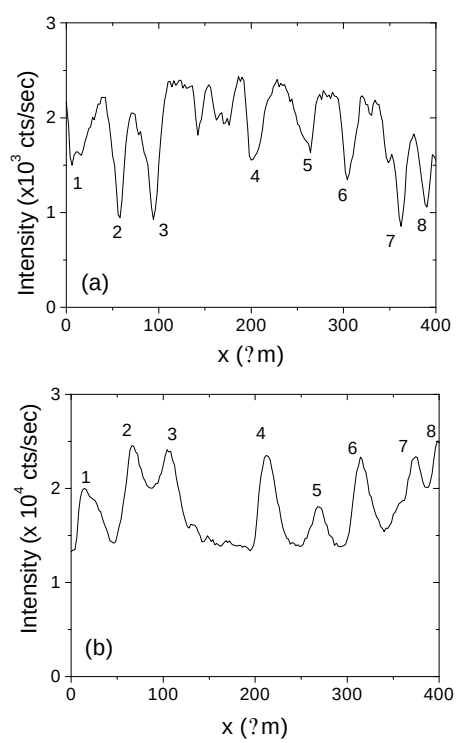

Figure 13: *Microdiffraction line scans taken at the 004 Bragg peak of (a) the SiGe (15%Ge) layer and (b) the Si substrate*

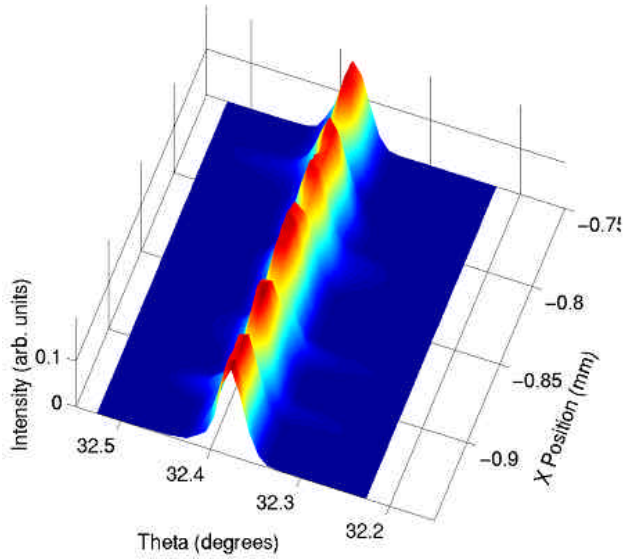

Figure 14: *Theta scans at intervals along the x direction for the layer sample shown in Figure 12.*

[17].

A plot of θ scans vs. x position for the same sample is shown in **Figure 14**. The unvarying center position of the θ scans implies that the film is well-oriented, with slight distortions where the pileups occur.

Figure 15 shows a SiGe(004) scanning topograph at fixed θ for a 98% relaxed $Si_{0.83}Ge_{0.17}$ film [7]. Comparing this to **Figure 12**, one can see that the much greater density of misfit dislocations decreases the amount of diffracting area. There are, however, rectangular areas that still meet the diffraction condition at the fixed θ angle of the sample.

A series of θ scans along the x direction, **Figure 16**, shows that local regions on the order of 10 – 20 μm diffract at different tilt angles [7]. Thus, the large pileups of misfit dislocations have resulted in tilted local regions between them. The range of tilt angles in this film is ~0.2 degrees.

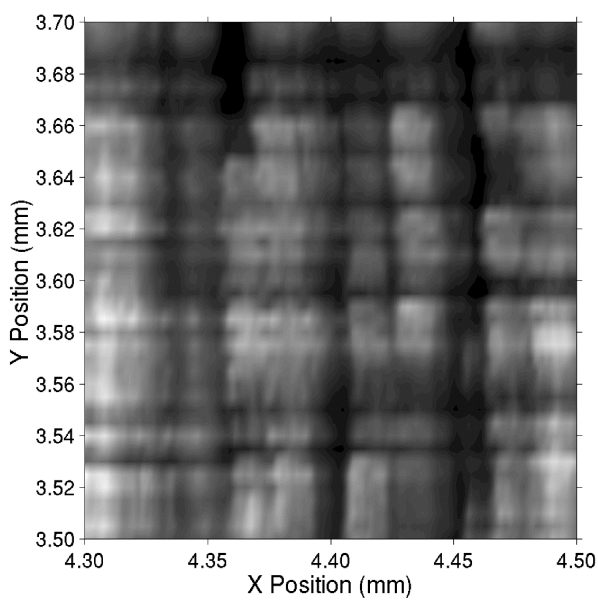

Figure 15: *Topograph of a 98% relaxed SiGe film.*

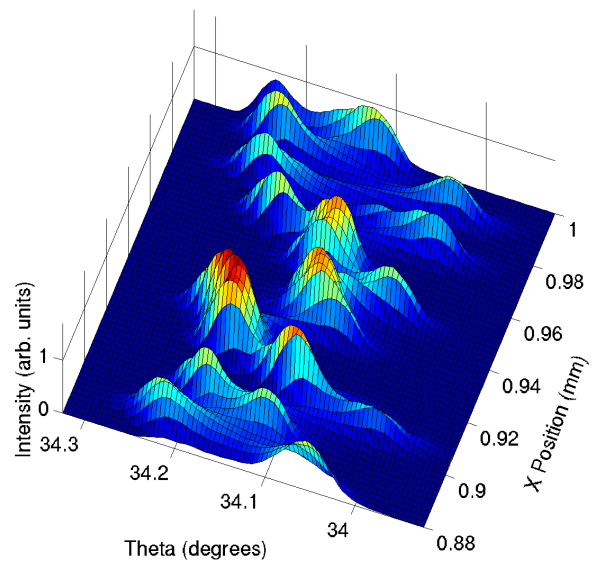

Figure 16: *Theta scans at intervals along the x direction for the layer sample shown in Figure 15.*

Summary

The X20 microbeam instrument was commissioned in 1997 and has served well as a specialized regional tool for IBM scientists to measure properties of microelectronics-related materials on the microns length scale. The use of a capillary optic to condense the x-ray beam comes with its own special set of advantages and disadvantages. The main advantages are low cost (if made in-house) and high divergence. The divergence of the beam makes it relatively easy to find grains and reflections from small crystallites or misoriented regions of a sample. However, this same divergence provides a challenge to accurately determine lattice spacings and optain a small illuminated area on the sample.

References

1. W. Yun, B. Lai, D. Shu, A. Khounsary, Z. Cai, J. Barraza, D. Legnini, "Design of a Dedicated Beamline for X-ray Microfocussing- and Coherence-Based Techniques at the Advanced Photon Source," *Rev. Sci. Instrum.*, **67** (9) (1995) CDROM

2. P. Deschamps, P. Engstrom, S. Fiedler, C. Riekel, S. Wakatsuki, P. Hogho, and E. Ziegler, "A Double Multilayer Monochromator at an ESRF Undulator for Microbeam Experiments," *J. Synchrotron Rad.* **2**, 124 (1995).

3. I.C. Noyan, J.L. Jordan-Sweet, E.G. Liniger, and S.K. Kaldor, "Microbeam Diffraction Studies of Interfacial Strain," *National Synchrotron Light Source Activity Report 1997,* E.Z. Rothman and J.B. Hastings, Eds., Brookhaven National Laboratory publication BNL-52540, New York, 1998, p.2-7.

4. I.C. Noyan, J. Jordan-Sweet, EG. Liniger, and S.K. Kaldor, "Characterization of Substrate/Thin- film Interfaces with X-ray Microdiffraction," *Appl. Phys. Lett*. **72**,3338-3340 (1998).

5. P.-C. Wang, I.C. Noyan, S.K. Kaldor, J.L. Jordan-Sweet, E.G. Liniger, and C.-K. Hu, "Topographic Measurement of Electromigration-induced Stress Gradients in Aluminum Conductor Lines," *Appl. Phys. Lett*. **76** (25), 3726 (2000).

6. P.-C. Wang, I.C. Noyan, S.K. Kaldor, J.L. Jordan-Sweet, E.G. Liniger, and C.-K. Hu, "Real-time X-ray Microbeam Characterization of Electromigration Effects in Al(Cu) Wires," *Appl. Phys. Lett.* **78** (18), 2712 (2001).

7. P.M. Mooney, J.L. Jordan-Sweet, I.C. Noyan, S.K. Kaldor, and P.-C. Wang, "Observation of Local Tilted Regions in Strain-relaxed SiGe/Si Buffer Layers Using X-ray Microdiffraction," *Appl. Phys. Lett.* **74** (5), 726 (1999).

8. P.M. Mooney, J.L. Jordan-Sweet, and S. Christiansen, "Scanning X-ray Microtopographs of Misfit Dislocations at SiGe/Si Interfaces," *Appl. Phys. Lett.* **79** (15), 2363 (2001).

9. I.C. Noyan, P.-C. Wang, S.K. Kaldor, and J.L. Jordan-Sweet, "Deformation Field in Single- crystal Semiconductor Substrates Caused by Metallization Features," *Appl. Phys. Lett*. **74**, 2352 (1999).

10. G.E. Ice and B.C. Larson, "Polychromatic X-ray Microdiffraction: Back to the Future to Study Fundamental Issues in Materials Science," *Advanced Photon Source Research* No. 4, 7 (2001); G.E. Ice, J.-S. Chung, W. Lowe, E. Williams, and J. Edelman, "Small-displacement Monochromator for Microdiffraction Experiments," *Rev. Sci. Instr*. **71**(5), 2001 (2000).

11. D.E. Eastman, C.B. Stagarescu, G. Xu, P.M. Mooiney, J.L. Jordan-Sweet, B. Lai, and Z. Cai, "Observation of Columnar Microstructure in Step-graded $Si_{1-x}Ge_x$/Si Films Using High-resolution X-ray Microdiffraction," *Phys. Rev. Lett.* **88**, 156101 (2002).

12. Eric G. Liniger, IBM Research Division, T.J. Watson Research Center, Yorktown Heights, NY.

13. I.C. Noyan, P.-C. Wang, S.K. Kaldor, J.L. Jordan-Sweet, and E.G. Liniger, "Divergence Effects in Monochromatic X-ray Microdiffraction Using Tapered Capillary Optics," *Rev. Sci. Instr.* **71**(5), 1991 (2000).